Acta Mech. Sin. (2017) 33(4):742–753
DOI 10.1007/s10409-017-0684-5

RESEARCH PAPER

Experimental investigation on the wake interference among wind turbines sited in atmospheric boundary layer winds

W. Tian[1,2] · A. Ozbay[2] · X. D. Wang[3] · H. Hu[2]

Received: 14 April 2017 / Revised: 20 April 2017 / Accepted: 26 April 2017 / Published online: 1 June 2017

Abstract We examined experimentally the effects of incoming surface wind on the turbine wake and the wake interference among upstream and downstream wind turbines sited in atmospheric boundary layer (ABL) winds. The experiment was conducted in a large-scale ABL wind tunnel with scaled wind turbine models mounted in different incoming surface winds simulating the ABL winds over typical offshore/onshore wind farms. Power outputs and dynamic loadings acting on the turbine models and the wake flow characteristics behind the turbine models were quantified. The results revealed that the incoming surface winds significantly affect the turbine wake characteristics and wake interference between the upstream and downstream turbines. The velocity deficits in the turbine wakes recover faster in the incoming surface winds with relatively high turbulence levels. Variations of the power outputs and dynamic wind loadings acting on the downstream turbines sited in the wakes of upstream turbines are correlated well with the turbine wakes characteristics. At the same downstream locations, the downstream turbines have higher power outputs and experience greater static and fatigue loadings in the inflow with relatively high turbulence level, suggesting a smaller effect of wake interference for the turbines sited in onshore wind farms.

✉ H. Hu
huhui@iastate.edu

[1] School of Aeronautics and Astronautics, Shanghai Jiao Tong University, Shanghai 200240, China

[2] Department of Aerospace Engineering, Iowa State University, Ames, IA 50011, USA

[3] School of Energy, Power and Mechanical Engineering, North China Electric Power University, Beijing 102206, China

Keywords Wind turbine aerodynamics · Turbine wake characteristics · Wake interference over wind farms · Dynamic wind loadings acting on wind turbines

1 Introduction

Wake interferences among multiple wind turbines in a modern wind farm have been found to affect their aeromechanic performance significantly. The velocity deficit recovery and turbulence intensity level enhancement are two very important aspects that characterize wake interferences among wind turbine arrays. The velocity deficits in the wakes of upstream wind turbines are closely related to the amount of the power that can be extracted by downstream turbines, while turbulence intensity levels in the wake flows are directly associated with the dynamic fatigue loadings acting on the downstream turbines. Depending on the wind turbine array spacing and layout, downstream wind turbines operating in a large wind farm were found to experience up to 40% power losses [1–3] and up to 80% more fatigue loads [4,5], due to the effects of wake interference.

To optimize the site design of array spacing and layout of wind turbine in wind farms, a good understanding of the turbine wake characteristics is very important for evaluating the effects of wake interference among wind turbine arrays. Better understanding has been obtained in recent years by both experimental and numerical studies of the characteristics of wind turbine wakes [6–12]. As described by Vermeer et al. [13], the wake flow behind a wind turbine can typically be divided into a near and a far wake. The far wake characteristics, which directly associate with the aeromechanic performance of downstream wind turbines in large arrays, are usually predicted by using turbine wake models, including kinematic models and added turbulence models.

Kinematic models are used to describe velocity deficits in the region influenced by wind turbine wake. One of the most widely used model is the Jensen wake model developed by Jensen [14]. The wake diameter in the Jensen model is given by:

$$D_{\mathrm{w}}(x) = D + 2kx, \tag{1}$$

where x is the distance from upstream wind turbine, D is the rotor diameter, and k is the wake expansion coefficient. Based on the empirical formula proposed by Frandsen [15], k can be obtained by:

$$k = \frac{0.5}{\ln(H/z_0)}, \tag{2}$$

where H and z_0 are the wind turbine hub height and surface roughness length. One can calculate the fully developed velocity in the wake as

$$u(x) = U_0\left[1 - \frac{1-\sqrt{1-C_{\mathrm{T}}}}{(1+2kx/D)^2}\right], \tag{3}$$

where C_{T} and U_0 are the thrust coefficient of the wind turbine and the incoming wind velocity.

It can be seen from Eq. (2) that the wake expansion coefficient is only related to the surface roughness length. In fact, wake expansion is affected by many factors, such as turbulence intensity in incoming atmospheric boundary layer (ABL) wind, atmospheric stability, and additional turbulence intensity caused by an upstream wind turbine. As indicated by Politis et al. [16], the presence of a wind turbine produces additional turbulence, which enhances the turbulence in the wake flow and accelerates the wake recovery rate. Similarly, Bastankhah and Porté-Agel [17] suggested that the complex vortex structures generated by the rotating turbine blades increases the turbulence intensity levels in the turbine wakes; therefore, the wake expansion coefficient, k, should also be increased accordingly.

Since the wake expansion coefficient, k, is related to the turbulence intensity level, the turbulence in the turbine wake should be estimated before k is corrected. The added turbulence intensity in the turbine wake, I_+, is predicted by several analytical models using the following definition

$$I_+ = \sqrt{I_{\mathrm{w}}^2 - I_0^2}, \tag{4}$$

where I_{w} and I_0 are the turbulence intensity in the turbine wake and the turbulence intensity in incoming ABL wind.

The wake added turbulence model as proposed by Quarton and Ainslie [18] is expressed as

$$I_+ = K_1 C_{\mathrm{T}}^{\alpha_1} I_0^{\alpha_2} (x/x_{\mathrm{n}})^{\alpha_3}, \tag{5}$$

Table 1 Parameters for the Quarton turbine wake models

	Wake added turbulence model			
	K_1	α_1	α_2	α_3
Quarton original model [18]	4.8	0.7	0.68	−0.57
Quarton alternative model [20]	5.7	0.7	0.68	−0.96

where x_{n} is the near wake length, which is defined by Vermeulen [19].

Later, Hassan [20] proposed an alternative turbine wake model based on the findings of wind tunnel tests. The parameters for the original and alternative models are given in Table 1.

Moreover, Crespo and Hernandez [21] suggested the following model to calculate the added turbulence intensity in the wake

$$I_+ = 0.73 a^{0.8325} I_0^{0.0325} (x/D)^{-0.32}. \tag{6}$$

The applicability of this model is $0.07 < I_0 < 0.14$, $0.1 < a < 0.4$, and $5 < x/D < 15$, where a is the axial induction factor.

It should be noted that C_{T} is used in Eq. (5), while a is used in Eq. (6). The relationship between C_{T} and a can be obtained as follow according to the actuator disk theory

$$C_{\mathrm{T}} = 4a(1-a). \tag{7}$$

While many investigations have been conducted in recent years to assess wind turbine wakes, most of them focused on offshore wind farms where wind turbine wake-induced power losses appear much larger than predicted a priori [22]. This finding is likely due to the low turbulence levels of offshore wind farms, which impede wake recovery. According to Barthelmie et al. [23], analysis of the data from onshore wind farms does not indicate as large a "deep array effect" as has been observed in offshore wind farms. It is also likely due to the difference in turbulence levels between onshore and offshore wind farms. In their work, Medici and Alfredsson [24] performed a wind tunnel study and indicated that the wake characteristics behind a model wind turbine can be significantly changed by the presence of turbulence in the incoming flow. Furthermore, Chamorro and Porté-Agel [25] carried out an experimental study to characterize in the wake flow behind a wind turbine model sited in a boundary layer wind tunnel with rough and smooth surfaces. They showed that the effect of inflow turbulence is not negligible even in the very far wake (i.e., at a downwind distance of $15D$). Wu and Porté-Agel [26] performed a large-eddy simulation (LES) to study the characteristics of turbine wakes

over homogeneous flat surfaces in ABL flows with four different roughness lengths. They found that the different inflow turbulence levels would lead to distinct effects on the wake characteristics, including mean velocity deficit, turbulence intensity, and turbulent shear stress. More recently, an experimental study performed by Tian et al. [27] reported the effects of inflow turbulence on the near wake structures and the dynamic wind loads of a model wind turbine placed in an ABL wind tunnel.

In the present study, an experimental investigation was conducted to examine the effects of incoming surface wind conditions on the characteristics of turbine wakes and the wake interference among upstream and downstream wind turbines sited in ABL winds. The experiments were conducted in a large-scale aerodynamic/atmospheric boundary layer (AABL) wind tunnel. A set of horizontal axis wind turbine (HAWT) models were mounted in the test section of the AABL wind tunnel. Two different types of the incoming boundary layer winds, i.e., one with a relatively low turbulence level in the incoming airflow to simulate the ABL winds over typical offshore wind farms, and the other with relatively high turbulence level to represent those over typical onshore wind farms, were generated in the AABL tunnel for a comparative study. Flow characteristics in the turbine wakes, including velocity deficits and turbulence intensity distributions, were measured by using a Cobra Probe Anemometry system. The measurement results of the present study were compared quantitatively against the predictions of the analytical wake models described above. The power outputs and dynamic loadings acting on wind turbine models were also monitored during the experiments. The detailed flow measurements were correlated with dynamic wind loadings and power output data for a better understanding about the effects of the inflow conditions on the turbine wake characteristics and wake interferences among upstream and downstream turbines in wind farm settings for the optimal spacing and layout design of wind farms.

2 Experimental setup and procedure

2.1 ABL wind tunnel

Experimental studies were conducted in the AABL wind tunnel at Iowa State University. The test section of the AABL wind tunnel is 20 m long, 2.4 m wide, and 2.3 m high. Figure 1 shows a picture of the test section of the AABL wind tunnel. During the experiments, different sizes and types of triangular spires and wooden blocks were placed on the floor at the entrance of the wind tunnel test section in order to generate different types of boundary layer winds to simulate different ABL winds over typical onshore and offshore wind farms. A zero pressure gradient condition was achieved for the development of the ABL winds by adjusting the ceiling of the AABL tunnel.

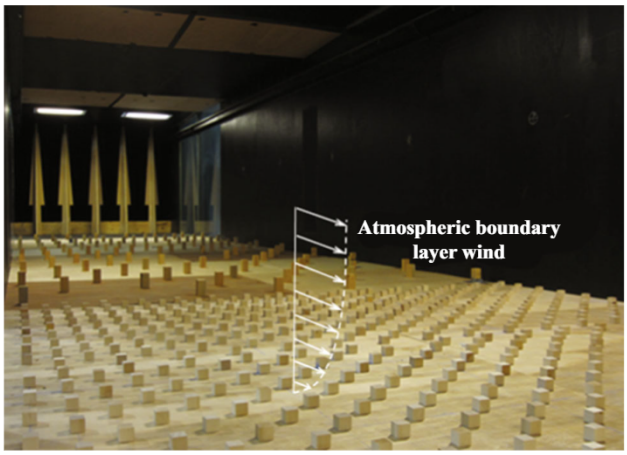

Fig. 1 Test section of the AABL tunnel used for the experimental study

Figure 2 shows the measured mean velocity and turbulence intensity profiles of two different types of boundary layer airflows generated inside the AABL tunnel at the locations where the wind turbine models would be mounted for the experimental study. By fitting the logarithmic law to the measured mean velocity profiles as shown in Fig. 2a, the friction velocity and the surface roughness lengths of the simulated ABL winds can be obtained [28]. For the low turbulence inflow case, the friction velocity and surface roughness length were found to be $u_* = 0.20$ m/s and $z_0 = 0.01$ mm, while the parameters for the high turbulence inflow case were $u_* = 0.30$ m/s and $z_0 = 0.30$ mm.

Figure 2b shows that the turbulence intensity at the turbine hub height ($z/H = 1$) for the low turbulence inflow case was approximately 10%, i.e., within the range of the field measurement results obtained by Hansen et al. [1] for typical offshore wind farms. For the inflow with high turbulence level, the turbulence intensity at the turbine hub height is about 18%, which is close to the turbulence intensity levels measured in an onshore wind farm as reported by Smith et al. [29]. As described by Tian et al. [27], while the incoming surface wind with low turbulence level could be used to represent the ABL wind over typical offshore farms, the surface wind with high turbulence level was used to simulate the ABL wind over typical onshore farms.

2.2 Tested wind turbine model

Figure 3 shows schematically the wind turbine model (three-blade HAWT design widely used in modern wind farms) used in this paper. The wind turbine model has a rotor with radius of $R = 140$ mm and a turbine hub with height of $H = 225$ mm. The ratio of the blade swept area to the wind

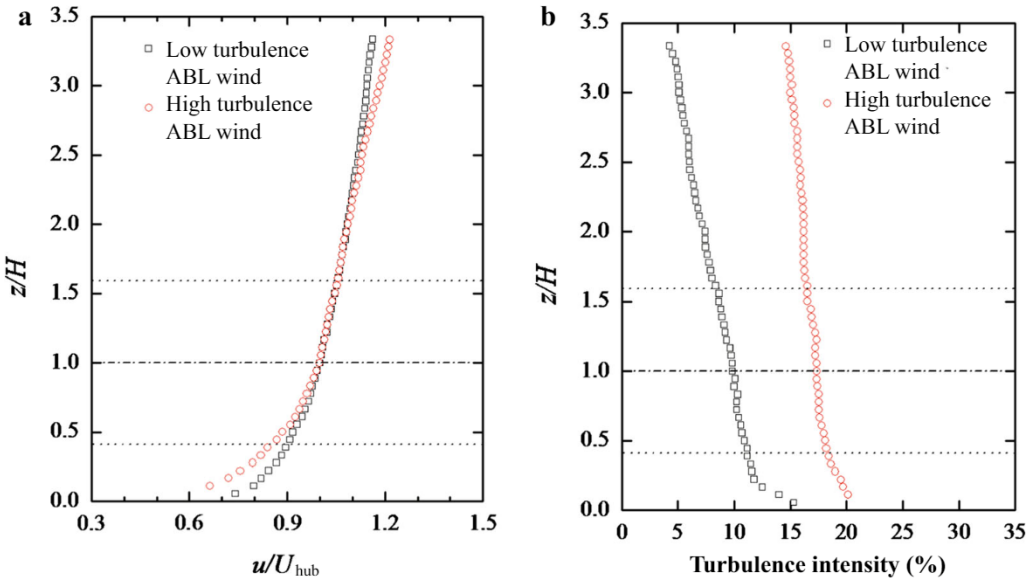

Fig. 2 Measured **a** streamwise mean velocity profiles and **b** turbulence intensity profiles of the boundary layer airflows inside the AABL tunnel. *Dotted lines top* and *bottom tip* height of the wind turbine model; *dash-dotted line* turbine hub height

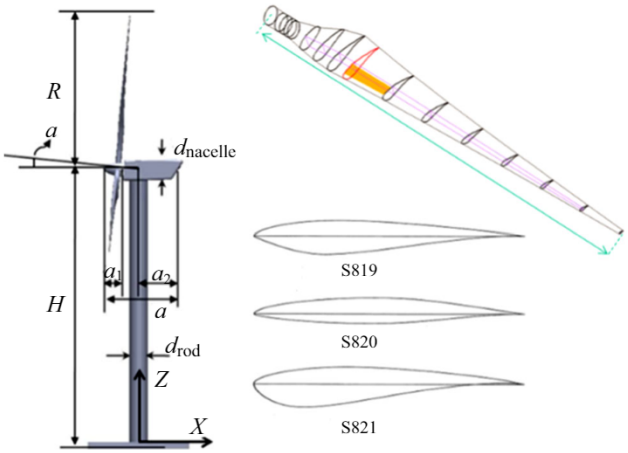

Fig. 3 Schematic diagram of the tested wind turbine models

tunnel area is approximately 1:110, which is small enough that the blockage effects of the test model for the wind tunnel testing can be neglected. The rotor of the tested wind turbine model consisted of three ERS-100 blades, which is developed by TPI Composites Inc. Further detailed information about the ERS-100 blade can be available in Ref. [30]. Similar wind turbine models were also used by Tian et al. [27] and Yuan et al. [31] for wind turbine aeromechanics studies.

During the experiments, the mean wind speed at the hub height of the model turbine was set to be about 5.0 m/s (i.e., $U_{\text{hub}} = 5.0$ m/s). As suggested by Chamorro et al. [32], the Reynolds number based on the turbine rotor diameter (D) and the flow velocity at the turbine hub height (U_{hub}), i.e., Re_D, was usually used to characterize turbine wake flows. The fundamental flow statistics (i.e., normalized profiles of mean velocity, turbulence intensity, kinematic shear stress, and velocity skewness) in the turbine wake flows would reach Reynolds number independence at a $Re_D \geqslant 9.0 \times 10^4$. The Reynolds number based on the turbine rotor diameter and the hub height velocity for the present study is about 90,000, which is in the range of the required minimum Reynolds number suggested by Chamorro et al. [32] in order to achieve Reynolds number independence of the turbine wake statistics. Further detailed statement about the Reynolds number effects on the wake characteristics and aeromechanic performances of wind turbine is available in Ref. [27].

2.3 Measurement of wake flow characteristics

A Cobra Probe Anemometry system (Turbulent Flow Instrumentation Pty Ltd) was used to measure the wake flow characteristics behind the wind turbine model. The Cobra Probe is a four-hole pressure probe, which is capable of measuring all three components of instantaneous flow velocity at a prescribed point at a sampling rate up to 2.5 kHz. Based on the time sequences of instantaneous measurement data of the flow velocity for 60 s, the ensemble-averaged flow quantities including mean velocity, turbulent kinetic energy, Reynolds shear stresses, and turbulence intensity can be derived. The uncertainty of the Cobra Probe for flow velocity measurement is $\pm$ 0.5%, the uncertainties for the measurements of ensemble-averaged flow quantities such as Reynolds stress and turbulence intensity are estimated to be within 2%. As shown schematically in Fig. 4, the flow characteristics measurements were taken in the symmetrical plate of the

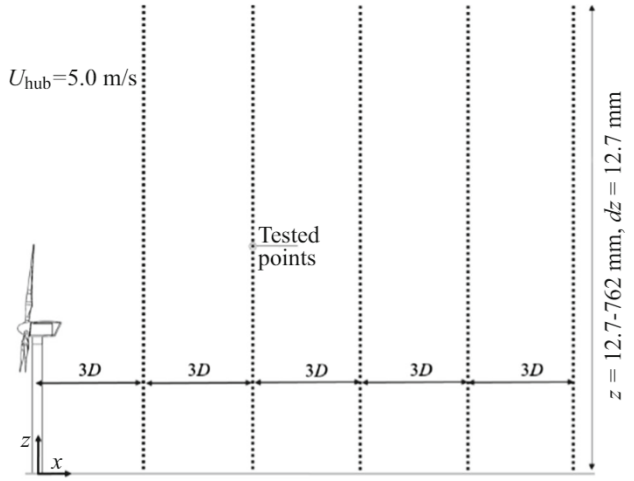

Fig. 4 Schematic of the measurement points in the turbine far wake (not scaled)

wind turbine (i.e., $y = 0$) at different downstream locations (i.e., $x/D = 3.0, 6.0, 9.0, 12.0, 15.0$). At each downstream location, the flow measurements were performed with the vertical coordinate ranging from $z = 12.7$ mm (i.e., 0.5 in) to $z = 762$ mm (i.e., 30.0 in) with the distance between the neighboring measurement points being $dz = 12.7$ mm (i.e., 0.5 in).

2.4 Measurement of dynamic wind load and power output

In addition to measuring wake flow characteristics, the power outputs and dynamic wind loadings of the upstream turbine, as well as the downstream wind turbines placed with different turbine spacing (i.e., $x/D = 3, 6, 9, 12, 15$) were also measured. For the dynamic wind loading measurements, aluminum rods, which were used as the towers of the wind turbine models, were connected to high-sensitivity load cells (JR3, model 30E12A-I40) through holes on the floor of the AABL tunnel. The JR3 load cell was mounted at the tower base of wind turbine model, which can provide instantaneous measurements of the forces and moment about all three axes. The uncertainty level of the JR3 load cell for force measurements was rated at ±0.25% of the full range (40 N).

During the experiments, the rotation speed of the wind turbine blades was measured by using a Tachometer (Monarch Instrument). By applying different electric loads to the electric circuits connected to the direct current (DC) generators installed inside the nacelles of the turbine models, the rotation speeds of the turbine blades were adjusted to 0–2200 rpm, and the corresponding tip speed ratio (TSR) of the model turbines was found to be in the range of 0–6.5. The power output of the model wind turbine (P) was determined based on the equation of $P = V^2/r$, where r is the electrical resistance that loads the electrical circuit, and V is voltage output of the DC generators. The voltage outputs of DC generators were acquired through a host computer via an A/D board (National Instruments) at a data sampling rate of 1.0 kHz for 180 s. The measurement uncertainty for the instantaneous voltage outputs were estimated to be within 5.0%. During the experiments, the power outputs and dynamic wind loads of the turbine models were measured with the turbine models operating at different TSRs. For the measurement results given in the present study, the wind turbine models were set to operate at their optimum TSRs (i.e., at the TSRs with the maximum power outputs).

3 Measurement results and discussions

3.1 Flow characteristics in the far wake

3.1.1 Mean velocity profiles in the turbine wake flows

It is well known that as the incoming airflow passes through the rotation disk of a wind turbine, a portion of the kinetic energy of the incoming airflow would be extracted by the wind turbine, resulting in velocity deficits in the wake behind the turbine. Figure 5 shows the normalized streamwise velocity profiles measured at different downstream locations behind a wind turbine model. The profiles of the incoming airflow were also plotted in the graphs for quantitative comparison. Since the velocity deficits were superimposed on the logarithmic distribution of the incoming flow velocity, a non-axisymmetric velocity distribution was observed in the wake flow behind the wind turbine model. High velocity deficits caused by the turbine rotor blades and nacelle in the region between the top and bottom blade tip heights can be observed clearly for both test cases with different incoming flow characteristics. Figure 6 gives the profiles of the "net" velocity deficits in the wakes behind the wind turbine model, which were obtained by subtracting the wake flow velocity from the incoming flow velocity (i.e., $\Delta u\,(z) = u\,(x, z) - U_\infty\,(z)$). It can be seen clearly that the distributions of the velocity deficits in the turbine wakes show approximately axisymmetric behavior, with the axis of symmetry located at the hub height. This axisymmetric behavior breaks down at the further downstream locations where the turbine wakes expand becoming wide enough to reach to the ground.

As shown in Figs. 5 and 6, a key difference between the two test cases with different incoming flow characteristics is that the wake flow would expend much faster and the velocity deficits would recover much more rapidly for the high turbulence inflow case (i.e., for the onshore wind farm scenario). As described in Ref. [27], the recovery rate of the velocity deficits are closely related to the turbulence levels in the turbine wakes. The high turbulence intensity levels in the wake

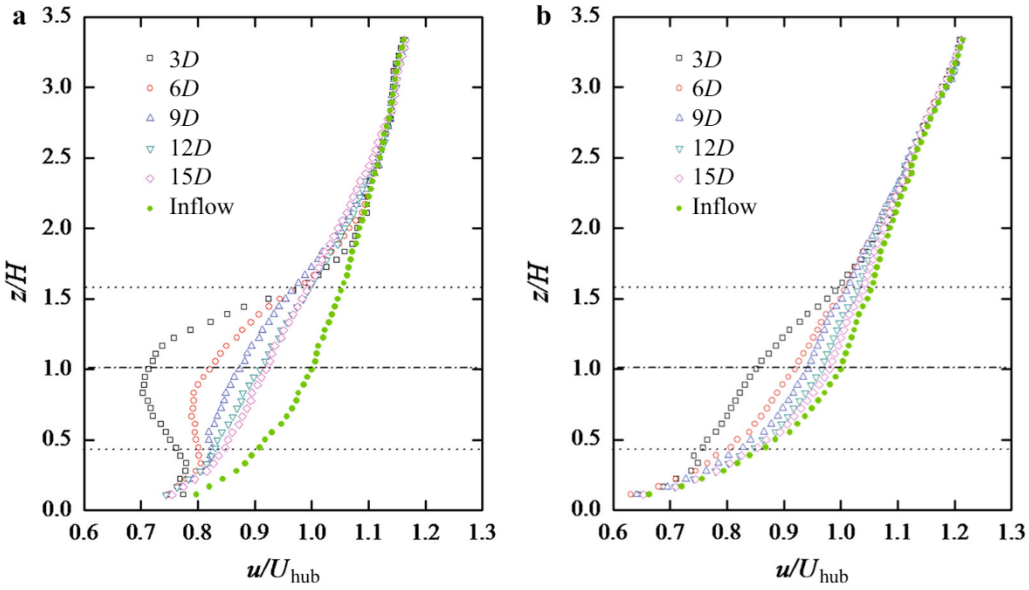

Fig. 5 Normalized mean streamwise velocity profiles at different downstream locations. **a** Low turbulence inflow case; **b** high turbulence inflow case

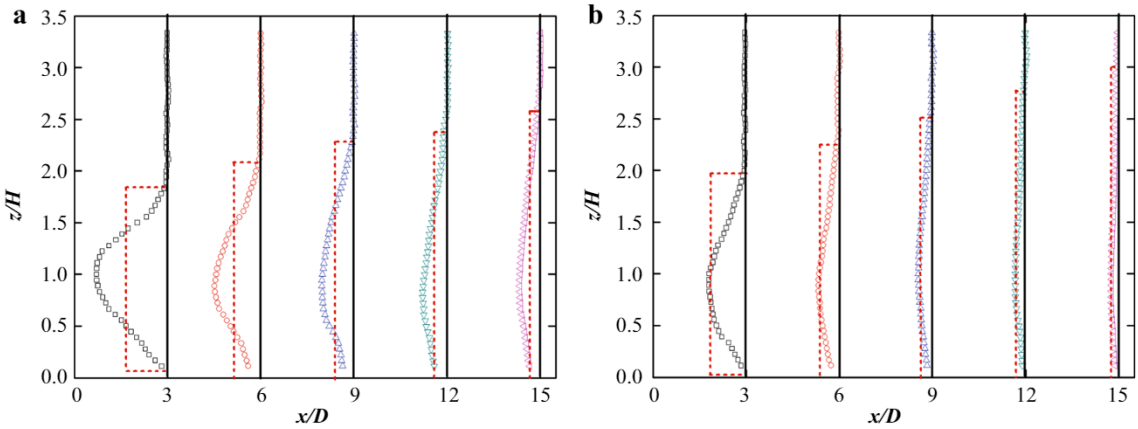

Fig. 6 Measured streamwise velocity deficits at different downstream locations in comparison with the predicted profiles of Jensen model [14]. **a** Low turbulence inflow case; **b** high turbulence inflow case

flows would play an important role in enhancing intensive flow mixing to promote the transport of kinetic energy in the turbine wakes, resulting in a much faster recovery of the velocity deficits in the turbine wakes.

The velocity deficits predicted by using the analytical turbine wake model suggested by Jensen [14] are also plotted in Fig. 6 as the dashed lines in the graphs for quantitative comparison. As mentioned above, Jensen model [14] is a one-dimensional analytical model, which assumes that the wind speed in the wake remains constant at a given downstream cross section. This assumption has a significant effect on the accuracy of power production estimation. Numerous studies have been performed to modify Jensen model by introducing different wake zones that provide a more accurate description of the turbine wake. For example, Tian et al. [33] proposed alternative approaches to modify the Jensen model by incorporating a Gaussian velocity profile that develops as a function of the downstream distance behind upstream the wind turbine.

As shown in Fig. 6, based on the comparisons of the measured and predicted velocity deficits in the turbine wakes, significant differences can be observed between the two test cases with different incoming flow conditions. For the low turbulence inflow case, the measured velocity deficits in the turbine wake were found to be much greater than the predicted values by using the Jensen model [14]. The underpredictions of the velocity deficits in the turbine wakes lead to an over-estimation of the power outputs for the downstream wind turbines sited in the turbine wakes, which was found to agree well with the field measurement data collected in

an offshore wind farm as reported in Ref. [22]. However, the predicted velocity deficits shown in Fig. 6b were found to be much closer to the measurement results for the high turbulence inflow case. The findings derived from the present study suggest that the incoming ABL wind characteristics significantly affect the wake recovery, which should be considered properly in the analytical turbine wake models in order to provide a better prediction of the turbine wake characteristics and more accurate estimation of the turbine power output.

Based on the measured velocity profiles in the turbine wake flows as those shown in Fig. 6, the expansion of the turbine wake as a function of the downstream locations, in the term of the evolution of the diameter of the turbine wake as called by Jensen model [14], can be determined. As mentioned above, the axisymmetric distribution of the "net" velocity deficits in the turbine wake would break down in the far wake region when the turbine wake interacts with the ground. Therefore, only the upper portions of the turbine wake (i.e., the wake region above the turbine hub height) were considered in determining the turbine wake diameter in order to eliminate the ground effects. In the present study, the turbine wake region is determined based on a criterion that the magnitude of the velocity deficits (Δu) on the boundary of the turbine wake is smaller than 0.05 m/s (i.e., $<1.0\%$ of the turbine hub height velocity).

Figure 7 shows the variations of the measured wake diameter as a function of the downstream distance away from the upstream turbine model for the test cases with two different incoming flow characteristics. The wake diameters predicted by using the Jensen model [14] are also given in the plots for comparison. It can be seen clearly that the turbine wake was found to expend much faster (i.e., have greater wake diameter values) for the test case with high turbulence levels in the incoming airflow (i.e., for the onshore wind farm case), in comparison with that of the low turbulence inflow case (i.e., for the offshore wind farm case). It can also be found that the wake diameters based on the experimental data of the present study would always be greater than those predicted by using the Jensen model [14], regardless of the turbulence levels of the incoming surface winds. As described in Refs. [16,17], it is likely caused by the presence of additional turbulence in the turbine wakes (i.e., the added turbulence as induced by the upstream wind turbines) that were not considered properly in the Jensen model [14]. The additional turbulence in the turbine wake would enhance the expansion of the turbine wakes and accelerate the recovery of the velocity deficits in the turbine wakes, causing the differences between the measured and predicted wake diameter values shown in Fig. 7. The characteristics of the added turbulence in the turbine wake induced by the upstream wind turbine and their impacts on the wake expansion and recovery of the velocity deficits in the turbine wakes will be further discussed in the next section.

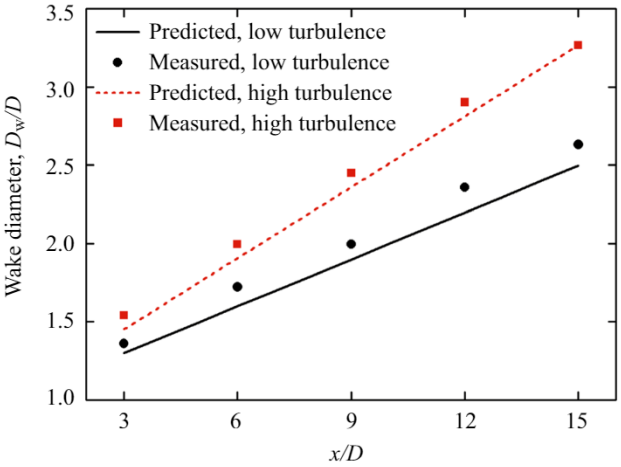

Fig. 7 Measured turbine wake diameters versus predictions of Jensen model [14]

3.1.2 Characteristics of the turbulence intensities in the turbine wakes

In comparison with those of the incoming surface winds, the turbulence intensity levels in the wake flows behind wind turbines were found to be enhanced greatly due to the existence of the upstream wind turbines. The enhanced turbulence intensity levels in the turbine wake flows would lead to increased fatigue loadings for the downstream wind turbines. Figure 8 shows the measured turbulence intensity distributions at different downstream locations in the turbine wakes for the test cases with two different turbulence levels in the incoming surface winds. It can be seen clearly that, unlike the velocity deficits being axisymmetrically distributed in the turbine wakes, the turbulence intensity distributions in the turbine wakes were found to be non-axisymmetric at all the downstream locations, regardless of the turbulence levels of the incoming surface winds. Such behavior is believed to be closely related to the non-uniformity of the turbulence levels in the incoming surface winds as shown in Fig. 2 and the presence of the ground. As reported by Hu et al. [11] and Tian et al. [27], due to the periodic shedding of the unsteady tip vortices, root vortices, and turbulent flow structures around the turbine nacelle, the turbulence intensity levels in the turbine wakes were found to enhanced greatly, especially in the region above the wind turbine hub. As described in Ref. [27], the dissipation of these complicated vortex structures with downstream distance is relatively slow for the test case with low turbulence inflow (i.e., offshore wind farm case), which leads to a slow decrease in the enhanced turbulence levels in the turbine wakes. As shown in Fig. 8a, the turbulence levels in the turbine wakes were found to be still much higher than those in the incoming surface even at the downstream location of $x/D = 15$. For the test case with high turbulence inflow (i.e., onshore wind farm case), the complicated wake

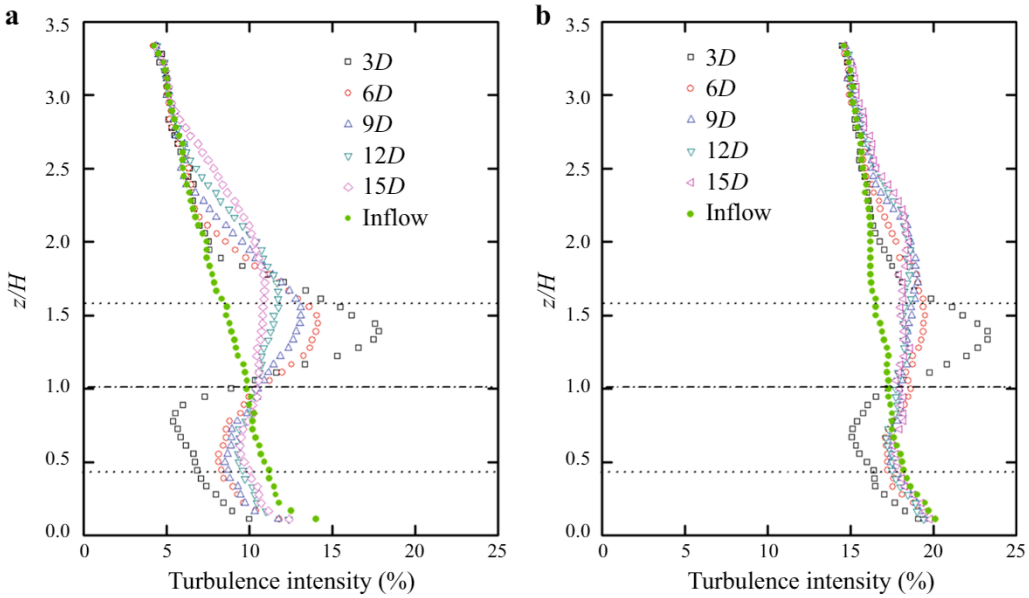

Fig. 8 Measured turbulence intensity profiles at different downstream locations. **a** Low turbulence inflow case; **b** high turbulence inflow case

vortex structures (i.e., the tip vortices, root vortices, and the unsteady vortices shedding from the turbine nacelle) would break down and dissipate quickly after being shed from the wind turbine model, as reported by Tian et al. [27]. As shown clearly in Fig. 8b, the added turbulence levels in the turbine wake were found to decrease dramatically and reach to a relatively low level as the downstream distance increasing from $x/D = 3.0$ to $x/D = 6.0$. Beyond the downstream distance of $x/D = 6.0$, the added turbulence levels in the turbine wakes for the test case with relatively high turbulence inflow were found to become much smaller, in comparison with those of the low turbulence inflow case. Similar findings were also reported by Wu and Porté-Agel [26]. It can also be seen that, unlike the region above the turbine hub with enhanced turbulence levels in the turbine wakes, the turbulence levels in the region near the ground was found to be reduced, in comparison to those in the incoming ABL winds. As described by Chamorro and Porté-Agel [25], such reduction of the turbulence intensities in the near ground region would be induced by the decreased mean shear and associated turbulent kinetic energy production of in the near ground region.

Following up the work described by Quarton and Ainslie [18] and Crespo and Hernandez [21], the mean values of the added turbulence intensity levels in the turbine wakes were calculated based on the measurement results of the present study. Similar to that used in determining the turbine wake diameters, only the measurement data at in upper portion of the turbine wakes (i.e., the wake region above the turbine hub height) were used to calculate the averaged values of the added turbulence intensity levels in the turbine wake in order

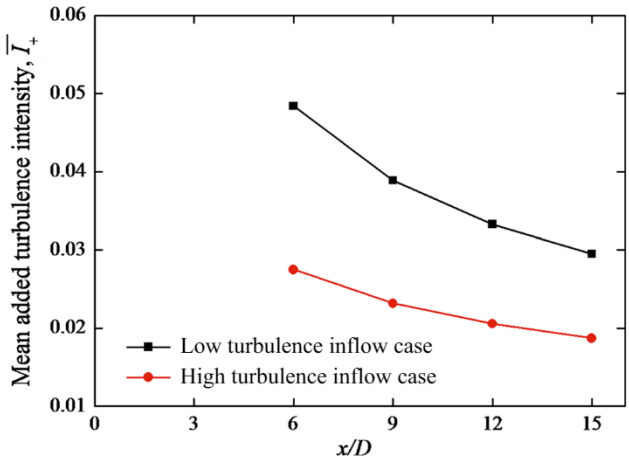

Fig. 9 Measured values of the added turbulence intensities at different downstream locations

to exclude the ground effect. In the present study, the averaged values of the added turbulence intensities in the turbine wakes at different downstream locations were calculated by using the following equation

$$\bar{I}_+ = \frac{1}{\pi R_w^2} \int_0^{R_w} I_+(r) 2\pi r \mathrm{d}r, \tag{8}$$

where R_w is the radius in the upper part of the turbine wake and $I_+(r) = I_+(z - H)$ for $H \leqslant z \leqslant (H + R_w)$.

Figure 9 shows the variations of the averaged values of the added turbulence intensities in the turbine wakes, $\bar{I}_+$, as a function of the downstream distance away from the upstream wind turbine model for the test cases with two dif-

ferent incoming flow characteristics. It can be seen clearly that for the test cases with low turbulence inflow (i.e., for the offshore wind farm scenario), the added turbulence intensity levels in the turbine far wake (i.e., $x/D = 6$–15) were found to be 3%–5%, which is comparable to the background turbulence levels (i.e., the turbulence levels of the incoming surface wind, which were about 6%–10% at the upper portion of the turbine model as shown in Fig. 2). Therefore, the added turbulence intensity induced by the upstream wind turbine would greatly affect the evolution of the turbine wakes. As shown clearly in Fig. 7, due to the effects of the added turbulence intensity in the turbine wake, which was not taken into account in the Jensen mode, the measured values of the turbine wake diameters were found to be much greater than those predicted by using the Jensen model [14]. However, for the test case with relatively high turbulence inflow, the magnitude of the added turbulence intensity levels in the turbine far wake was found to be only ~2%, which is much smaller than the background turbulence levels (i.e., the turbulence levels in the incoming surface winds, which were about 16%–18% at the upper portion of the turbine model as shown in Fig. 2). As a result, the evolution of the turbine wake characteristics, including the wake expansion and recovery of the velocity deficits, would be mainly determined by the background turbulent levels in the turbine wake flows. Therefore, as shown clearly in Figs. 6 and 7, the predicted values of the velocity deficits and turbine wake diameters were found to agree with the measurement result reasonably well for the test case with relatively high turbulence inflow (i.e., for onshore wind farm scenario).

By examining the change rates of the added turbulence intensity levels along with increasing downstream distance as shown in Fig. 9, it was found that the decay profiles of the added turbulence intensities in the turbine far wake of $6 \leqslant x/D \leqslant 15$ could be fitted well by using power functions. The power exponents were found to be about –0.54 for the low turbulence inflow case and –0.42 for the high turbulence inflow case. The findings derived from measurement results of the present study were found to agree well with those reported in the previous studies of Quarton and Ainslie [18], Crespo and Hernandez [21], and Chamorro and Porté-Agel [25] about the turbulence characteristics in the turbine far wakes.

3.2 Effects of wake interference on the downstream turbines performance

3.2.1 Power output

Normalized power output of the downstream turbine model varying with the spacing between the upstream and downstream turbines (x/D) was plotted in Fig. 10. It shows that, corresponding to high velocity deficits in the wake flows behind the upstream wind turbine (Fig. 5), the downstream turbine has much less power output than the upstream turbine, due to the ingestion of the low-momentum wake flow of the upstream wind turbine. For the downstream turbine model sited at ~3D away from the upstream turbine, the wake interferences caused ~45% power losses in the inflow with low turbulence level and 30% in the inflow with high turbulence level. Since the velocity deficits in the turbine wakes recover gradually, the power losses of the downstream wind turbine caused by wake interference continuously decrease with increasing space between the upstream and downstream turbines. A distinct difference can be observed between the two test cases with different incoming flow characteristics, which were also found to be correlated very well with the measured velocity profiles in the turbine wakes given in Fig. 5. The downstream wind turbine in the inflow with high turbulence level always has higher normalized power outputs than the one with low turbulence level, since its velocity deficits in the turbine wake has a much faster recovery. The biggest difference in power outputs for the two compared case was found to appear with the downstream turbine mounted at the downstream location of $x/D = 6$, where the power output of the downstream turbine with high turbulence level is approximately 30% higher than that with low turbulence level. While the difference becomes smaller as the turbine spacing increases, it still retains approximately 16.5% higher than the case with low turbulence level, for the downstream turbine mounted at the downstream location of $x/D = 15$.

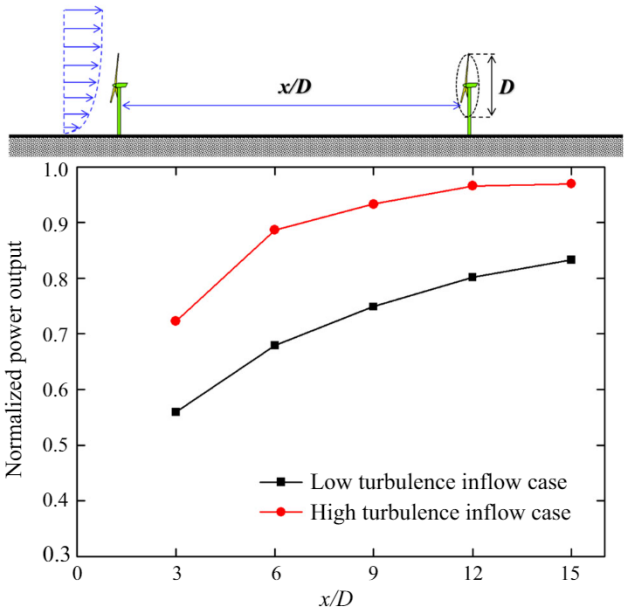

Fig. 10 Power outputs of the downstream turbine at different downstream locations

As revealed clearly in Fig. 10, for the downstream wind turbine located at $x/D = 12$, the inflow case with low turbu-

Table 2 Dynamic wind loads acting on the wind turbine models under different test conditions

	Upstream turbine	Downstream turbine				
		$3D$	$6D$	$9D$	$12D$	$15D$
Low turbulence inflow case						
Mean thrust coefficient, C_T	0.470	0.312	0.352	0.378	0.394	0.403
Standard deviation of thrust coefficient, σ_{C_T}	0.141	0.193	0.175	0.169	0.163	0.158
High turbulence inflow case						
Mean thrust coefficient, C_T	0.511	0.390	0.455	0.472	0.486	0.488
Standard deviation of thrust coefficient, σ_{C_T}	0.232	0.282	0.252	0.244	0.238	0.236

lence level has a power loss of ∼25%, which agrees well with the field measurements over an offshore wind farm conducted by Barthelmie et al. [2]. For the inflow having high turbulence level, the normalized power output of the downstream turbine sited at $x/D = 12$ was found to be approximately 0.95, which reaches almost the same level as the power output of the undisturbed upstream turbine. As suggested by Tian et al. [27], for the incoming surface winds with higher turbulence levels (i.e., onshore wind farms), enhanced turbulent mixing occurs in the turbine wake flows promote the kinetic energy transport by entraining more of the high-speed surrounding airflow to recharge the low-momentum wake flows behind the upstream turbines, thereby facilitating the velocity deficit recovery in the turbine wakes. As a result, compared to offshore wind farms with incoming ABL winds of low turbulence levels, onshore wind forms can produce much greater power outputs by placing the downstream wind turbines in the incoming ABL winds of higher turbulence levels.

3.2.2 Dynamic wind loads

The dynamic wind loadings acting on wind turbines are very important aspects for the mechanical design of wind turbines, as they would greatly affect the fatigue lifetimes of wind turbines. In the present study, the dynamic wind loadings acting on the wind turbine models under different test cases were also measured in order to evaluate the effects of the incoming flow characteristics on the dynamic wind loadings acting on the wind turbines in wind farm settings. Here we only measure the thrust coefficients, C_T, for conciseness. The thrust coefficient is defined as $C_T = \frac{T}{\frac{1}{2}\rho U_{hub}^2 \pi R^2}$, where T is the thrust acting on the wind turbine model, ρ is the air density, U_{hub} is the incoming wind velocity at the turbine hub height, and R is the radius of the wind turbine rotor. During the experiments, the thrust force was acquired for 120 s at the sample rate of 1000 Hz.

We measured the mean values (indicating the static wind loadings) and standard deviations (representing the fatigue wind loadings) of the dynamic wind loadings acting on the wind turbine models by using the time sequences of the instantaneous dynamic wind loading measurements. Table 2 summarizes the mean thrust coefficients and their standard deviations for the downstream turbine under different test conditions. The dynamic wind loadings acting on the upstream turbines are also listed in the table for comparison.

It is well known that a wind turbine's power output is proportional to the wind speed cubed at the turbine hub height, and the mean wind loadings acting on the wind turbine would be proportional to the square of the hub height velocity. Therefore, as listed in Table 2, the variations of mean wind loadings acting on the downstream turbine are tightly connected to the wake flow characteristics behind the upstream turbine, which have very similar behaviors as those of the measured power output data discussed above.

To optimize the mechanical design of wind turbines, more and more attention is paid to dynamic wind loadings because of its close relationship to the fatigue lifetime of wind turbines. As shown clearly in Table 2, the fatigue loadings acting on the wind turbine models (i.e., standard deviation values of the instantaneously measured wind loadings, σ_{C_T}) were found to be correlated well with the characteristics of the measured turbulence intensity distributions in the turbine wakes as those shown in Fig. 8. Higher fatigue loadings acting on both the upstream and downstream turbines were found in the inflows with high turbulence levels than those with low turbulence levels. It can also be seen in the inflow with low turbulence level that compared to turbulence acting on the upstream wind turbine, due to the wake interference effects from the upstream turbine, the fatigue loadings acting on the downstream turbine increase ∼37% (with $x/D = 3.0$) and ∼12% (with $x/D = 15.0$). The increase percentages are much greater than those in the inflow with high turbulence level (i.e., ∼20% at $x/D = 3.0$ downstream and only ∼2% at $x/D = 15.0$ downstream). Such features were found to be consistent with the behaviors of the added turbulence intensity levels in the turbine wakes described above.

4 Conclusion

Incoming surface wind effects on turbine wake characteristics and wake interference among upstream and downstream

winds turbines sited in ABL winds were experimentally examined in a large-scale ABL wind tunnel available at Iowa State University. Two types of incoming surface winds with distinct mean and turbulence characteristics were investigated, simulating the wind turbines operating in typical onshore/offshore wind farms. In addition to power outputs and dynamic wind loads, we also studied the characteristics in the wake flows behind the turbine models.

The experimental results show that the turbulence levels of incoming surface winds play a crucial role in determining the characteristics of the wake flows behind wind turbines. A higher turbulence level results in enhanced turbulent mixing in turbine wake flows and causes a much faster recovery of the velocity deficits in the turbine wakes. We also compared quantitatively experimental results against the predictions of the analytical wake models proposed in previous studies. This suggests that the effects of the incoming flow conditions (especially the turbulence intensity levels) should be considered properly in the turbine wake models for more accurate predictions of turbine wake characteristics.

The power measurement results reveal clearly that compared to the upstream turbines, the downstream turbines have much less power outputs because the low-momentum wake flows induced by upstream wind turbines. The turbulence levels of the incoming ABL winds were found to affect the power losses due to wake interference greatly. Even though they are mounted at the same downstream locations behind the upstream turbines, the downstream turbines in the inflow with higher turbulence levels have much higher power outputs than those with lower turbulence levels. More specifically, for $x/D = 3.0$ downstream, the wake interference causes a high power loss of the downstream up to $\sim$45% for the inflow with low turbulence level and $\sim$30% for the inflow with high turbulence level. When the downstream turbine was moved to $x/D = 12$ downstream, the power loss due to the wake interference was found to become less than 5% for the high turbulence inflow case (i.e., for onshore wind farms scenario). The corresponding power loss was still found to be as high as 25% for the low turbulence inflow case (i.e., for offshore wind farms scenario).

Dynamic wind loadings acting on the wind turbines were found to be tightly connected to the flow characteristics approaching the wind turbines. Corresponding to the higher power outputs, the downstream turbines would also experience higher static and fatigue wind loadings for the test case with high turbulence levels in the incoming flows. The increase of the fatigue loadings acting on the downstream turbine due to the wake interference was found to be more significant for the test case with low turbulence inflow (i.e., offshore wind farm scenario) than that of the high turbulence inflow case (i.e., onshore wind farm scenario). In summary, the findings of the present study suggest that the effects of the wake interference on the aeromechanic performance of the downstream wind turbines would be smaller in onshore wind farms than those in offshore wind farms, which agree well with those reported in previous field studies.

Acknowledgements The authors want to thank the funding support from the National Science Foundation (NSF) (Grants CBET-1133751 and CBET-1438099). Wei Tian also wants to thank the support from the National Key Technology Support Program of China (Grant 2015BAA06B04) and Shanghai Natural Science Foundation (Grant 16ZR1417600).

References

1. Hansen, K.S., Barthelmie, R.J., Jensen, L.E., et al.: The impact of turbulence intensity and atmospheric stability on power deficits due to wind turbine wakes at Horns Rev wind farm. Wind Energy **15**, 183–196 (2012)
2. Barthelmie, R.J., Folkerts, L., Ormel, F., et al.: Offshore wind turbine wakes measured by SODAR. J. Atmos. Ocean Technol. **20**, 466–477 (2003)
3. Adaramola, M., Krogstad, P.: Experimental investigation of wake effects on wind turbine performance. Renew. Energy **36**, 2078–2086 (2011)
4. Van Binh, L., Ishihara, T., Van Phuc, P., et al.: A peak factor for non-Gaussian response analysis of wind turbine tower. J. Wind Eng. Ind. Aerodyn. **96**, 2217–2227 (2008)
5. Sanderse, B.: Aerodynamics of Wind Turbine Wakes: Literature Review. Energy Research Center of the Netherlands. ECN-E-09-016 (2009)
6. Ross, J.N., Ainslie, J.F.: Wake measurements in clusters of model wind turbines using laser Doppler anemometry. In: Proceedings of the Third BWEA Wind Energy Conference Cranfield, UK, 172–184 (1981)
7. Barthelmie, R.J., Jensen, L.E.: Evaluation of wind farm efficiency and wind turbine wakes at the Nysted offshore wind farm. Wind Energy **13**, 573–586 (2010)
8. Wu, Y.: Large-eddy simulation of wind-turbine wakes: evaluation of turbine parametrizations. Bound. Layer Meteorol. **138**, 345–366 (2011)
9. Xie, S., Archer, C.: Self-similarity and turbulence characteristics of wind turbine wakes via large-eddy simulation. Wind Energy **18**, 1815–1838 (2015)
10. Sescu, A., Meneveau, C.: Large-eddy simulation and single-column modeling of thermally stratified wind turbine arrays for fully developed, stationary atmospheric conditions. J. Atmos. Ocean Technol. **32**, 1144–1162 (2015)
11. Hu, H., Yang, Z., Sarkar, P.: Dynamic wind loads and wake characteristics of a wind turbine model in an atmospheric boundary layer wind. Exp. Fluids **52**, 1277–1294 (2011)
12. Howard, K.B., Singh, A., Sotiropoulos, F., et al.: On the statistics of wind turbine wake meandering: an experimental investigation. Phys. Fluids **27**, 075103 (2015)
13. Vermeer, L., Sørensen, J., Crespo, A.: Wind turbine wake aerodynamics. Prog. Aerosp. Sci. **39**, 476–510 (2003)
14. Jensen, N.O.: A note on wind generator interaction. Technical Report Risø-M-2411, Risø (1983)
15. Frandsen, S.: On the wind speed reduction in the center of large clusters of wind turbines. J. Wind Eng. Ind. Aerodyn. **39**, 251–265 (1992)
16. Politis, E.S., Prospathopoulos, J., Cabezon, D., et al.: Modeling wake effects in large wind farms in complex terrain: the problem, the methods and the issues. Wind Energy **15**, 161–182 (2011)

17. Bastankhah, M., Porté-Agel, F.: A new analytical model for wind-turbine wakes. Renew. Energy **70**, 116–123 (2014)
18. Quarton, D., Ainslie, J.: Turbulence in wind turbine wakes. J. Wind Eng. **14**, 15–23 (1989)
19. Vermeulen, P.: An experimental analysis of wind turbine wakes. In: Third International Symposium on Wind Energy Systems, BHRA, 431–450 (1980)
20. Hassan, U.: A wind tunnel investigation of the wake structure within small wind turbine farms. E/5A/CON/5113/1890. UK Department of Energy, ETSU (1992)
21. Crespo, A., Hernandez, J.: Turbulence characteristics in wind turbine wakes. J. Wind Eng. Ind. Aerodyn. **61**, 71–85 (1996)
22. Barthelmie, R.J., Hansen, K., Frandsen, S.T., et al.: Modelling and measuring flow and wind turbine wakes in large wind farms offshore. Wind Energy **12**, 431–444 (2009)
23. Barthelmie, R.J., Pryor, S.C., Frandsen, S.T., et al.: Quantifying the impact of wind turbine wakes on power output at offshore wind farms. J. Atmos. Ocean Technol. **27**, 1302–1317 (2010)
24. Medici, D., Alfredsson, P.: Measurement on a wind turbine wake: 3D effects and bluff body vortex shedding. Wind Energy **9**, 219–236 (2006)
25. Chamorro, L., Porté-Agel, F.: A wind-tunnel investigation of wind-turbine wakes: boundary-layer turbulence effects. Bound. Layer Meteorol. **132**, 129–149 (2009)
26. Wu, Y., Porté-Agel, F.: Atmospheric turbulence effects on wind-turbine wakes: an LES study. Energies **5**, 5340–5362 (2012)
27. Tian, W., Ozbay, A., Hu, H.: Effects of incoming surface wind conditions on the wake characteristics and dynamic wind loads acting on a wind turbine model. Phys. Fluids **26**, 125108 (2014)
28. Zhou, Y., Kareem, A.: Definition of wind profiles in ASCE 7. J. Struct. Eng. **128**, 1082–1086 (2002)
29. Smith, C.M., Barthelmie, R.J., Pryor, S.C.: In situ observations of the influence of a large onshore wind farm on near-surface temperature, turbulence intensity and wind speed profiles. Environ. Res. Lett. **8**, 34006 (2013)
30. Locke, J., Valencia, U., Ishikawa, K.: Design studies for twist-coupling wind turbine blades. Sandia National Laboratories, Technical Report SAND 2004–0522 (2004)
31. Yuan, W., Tian, W., Ozbay, A., et al.: An experimental study on the effects of relative rotation direction on the wake interferences among tandem wind turbines. Sci. China Phys. Mech. Astron. **57**, 935–949 (2014)
32. Chamorro, L.P., Arndt, R.E.A., Sotiropoulos, F.: Reynolds number dependence of turbulence statistics in the wake of wind turbines. Wind Energy **15**, 733–742 (2012)
33. Tian, L., Zhu, W., Shen, W., et al.: Development and validation of a new two-dimensional wake model for wind turbine wakes. J. Wind Eng. Ind. Aerodyn. **137**, 90–99 (2015)